



1 **Eurasian snow depth in long-term climate**
2 **reanalyses**

3

4 Martin **Wegmann**^{1,2,3}, Yvan **Orsolini**⁴, Emanuel **Dutra**⁵, Olga **Bulygina**⁶,
5 Alexander **Sterin**⁶ and Stefan **Brönnimann**^{2,3}

6 ¹ *Institut des Géosciences de l'Environnement, University of Grenoble, France*

7 ² *Oeschger Centre for Climate Change Research, University of Bern, Switzerland*

8 ³ *Institute of Geography, University of Bern, Switzerland*

9 ⁴ *NILU—Norwegian Institute for Air Research, Kjeller, Norway*

10 ⁵ *ECMWF European Centre for Medium-Range Weather Forecasts, Reading, UK*

11 ⁶ *All-Russian Research Institute of Hydrometeorological Information—World Data*
12 *Centre, Obninsk, Russian Federation*

13

14 *Corresponding Author:*

15 *Martin Wegmann, martin.wegmann@univ-grenoble-alpes.fr*

16

17

18

19

20



21 **Abstract**

22 Snow cover variability has significant effects on local and global climate evolution.
23 By changing surface energy fluxes and hydrological conditions, changes in snow
24 cover can alter atmospheric circulation and lead to remote climate effects. To analyze
25 such multi-scale climate effects, atmospheric reanalysis and derived products offer the
26 opportunity to analyze snow variability in great detail far back in time. So far only
27 little is know about their quality. Comparing four long-term reanalysis datasets with
28 Russian in situ snow depth data, a good representation of daily to sub-decadal snow
29 variability was found. However, the representation of pre-1950 inter-decadal snow
30 variability is questionable, since datasets divert towards different base states. Limited
31 availability of independent long-term snow data hinders investigating this bifurcation
32 of snow states in great detail, but initial investigations reveal a non-stationary
33 performance of snow evolution representation. This study demonstrates the ability of
34 long-term reanalysis to reproduce snow variability accordingly.

35
36
37
38
39
40
41
42
43
44
45
46
47



48 1. Introduction

49 Snow is an important component of the climate system over the mid- and high-
50 latitude regions of the Earth. Its high shortwave albedo and low heat conductivity
51 alters heat and radiation fluxes at the Earth's surface and thus directly modulates
52 regional temperature evolution and ultimately atmospheric circulation patterns
53 (Barnett et al. 1988, Cohen and Rind 1991, Callaghan et al. 2011, Cohen et al. 2014).
54 Moreover, because snow acts as a temporary water reservoir, snow variability impacts
55 soil moisture, evaporation and ultimately precipitation processes (Yasunari et al.
56 1991).

57 As a result, snow cover has an essential influence on ecological (Jonas et al. 2008,
58 Peñuelas et al. 2009) and economical systems (eg. Agrawala 2007). Vice versa, snow
59 cover itself is determined by climate variations. Recent Arctic warming severely
60 impacted spring snow cover. Between 1979 to 2011, Arctic April snow cover extent
61 decreased at a rate of -17.8% per decade (Derksen and Brown 2012). In contrast,
62 regional snow cover increase in autumn over Eurasia was found in connection with
63 low Arctic sea ice concentration (Honda et al. 2009, Park et al. 2013, Wegmann et al.
64 2015), indicating the complexity of global and regional processes leading to snow
65 cover changes.

66 Reciprocally, as a slowly varying component of the climate system, the snow cover
67 influences large-scale climate patterns, and has been tapped as a source of
68 predictability at the subseasonal-to-seasonal scale, especially over Eurasia in autumn
69 and winter (Cohen and Entekhabi 1999, Jeong et al. 2013, Orsolini et al. 2013, Wu et
70 al. 2014, Ye et al. 2015,).

71 Therefore, large-scale monitoring and quantifying of snow cover is crucial for
72 assessing climate change and its representation in climate models (eg. Frei and Gong
73 2005, Brown and Mote 2009, Brown and Robinson 2011, Liston and Hiemstra 2011,
74 Ghatak et al. 2012, Zuo et al. 2015) and for analyzing cryosphere-climate feedbacks
75 (eg. Flanner et al. 2011, Orsolini and Kvamstø 2009, Zhang et al. 2013). Here we
76 analyze snow depths in climate in comparison to in-situ data, with the aim to better
77 assess cryosphere-atmosphere coupling processes in the context of the 20th century
78 climate evolution.



79 To this end, reanalysis products provide a compromise between the high temporal
80 resolution and length of in-situ observational datasets (eg. Bulygina et al. 2010) and
81 the large spatial coverage of satellite products (Siljamo and Hyvärinen 2011, Frei et al.
82 2012, Hüsler et al. 2014). Comprehensive reanalyses datasets are well suited to
83 investigate processes and mechanisms, and a variety of reanalyses are now routinely
84 produced by meteorological prediction centers, covering not only the satellite era but
85 also extending further back in time, such as (but not limited to) NCEP-DOE, ERA-40
86 and ERA-Interim, and JRA-25 and JRA-55 (e.g. Uppala et al. 2005, Onogi et al. 2007,
87 Compo et al. 2011, Dee et al. 2011, Rienecker et al. 2011, Poli et al. 2013).

88 However, so far only a few studies analyzed snow representation in reanalysis
89 products. Khan et al. (2008) compared measured snow data with snow water
90 equivalents and snow depth in the NCEP-DOE (Kanamitsu et al. 2002), ERA-40
91 (Uppala et al. 2005) and JRA-25 (Onogi et al 2007) reanalysis products over Russian
92 river basins. They found that the ERA-40 outperformed the NCEP-DOE and JRA25
93 in terms of correlations and mean values. Despite reproducing well the seasonal
94 variability, all reanalysis products struggled with snowmelt season values. Brown et al.
95 2010 compared ERA-40 and NCEP/NCAR snow cover extent to satellite and in-situ
96 datasets. They found that for the period 1982-2002 ERA-40 shows higher correlations
97 and smaller root mean squared errors (RMSE) than the NCEP reanalysis, and that
98 May values were considerably better approximated than June values. Brun et al. 2013
99 forced the CROCUS snow model with atmospheric conditions from ERA-INTERIM
100 (1970-1993) and found very high agreements with Eurasian in-situ snow
101 measurements. However, no snow output from the reanalysis directly was evaluated.

102 In addition, climate reanalyses extending back to the beginning of the 20th century or
103 earlier have now been produced for multi-decadal climate studies. Contrarily to the
104 above-mentioned reanalyses, these climate reanalyses, namely the 20th Century
105 Reanalysis (20CRv2) (Compo et al. 2011) and ERA-20C (Poli et al. 2016), solely rely
106 on assimilation of surface data. Even fewer studies have tried to quantify snow cover
107 extent and depth and their potential impact on climate in such centennial reanalyses.
108 Recently, Peings et al. 2013 compared in-situ snow measurements over Russia with
109 20CRv2 for the whole 20th century, and found that it consistently and realistically
110 represents the onset of Eurasian snow cover. However, the authors only investigated



111 the snow dataset in a binary fashion (snow/no snow).

112 Given the lack of inter-comparison studies of snow depth between reanalyses
113 products, we evaluate snow depth in four centennial state-of-the-art reanalyses. The
114 goal of this study is to assess the consistency between in-situ observations and
115 reanalyses estimation of snow depths. To assess this performance, we focus on early
116 snowfall season (October, November) and early snow melt season (April). Land
117 reanalyses will also be used in the assessment.

118 This article is structured as follows. Section 2 gives an overview of the various
119 datasets analyzed, whereas Section 3 defines the methods used in the comparison.
120 Section 4 presents the results for the evaluation. After discussing the results in Section
121 5, conclusions are drawn in Section 6.

122 **2. Data**

123 In this study, we use six different climate reanalysis datasets, which can be divided
124 into two families, namely the European Centre for medium-range Weather Forecasts
125 (ECMWF) products and the NOAA-CIRES Twentieth Century Reanalysis products.
126 These datasets are compared with Russian in-situ snow depth measurements.

127 **2.1 Reanalysis Datasets**

128 The Twentieth Century Reanalysis Version 2 (20CRv2) dataset allows retrospective
129 4-dimensional analysis of climate and weather between 1871 and 2012 (Compo et al.
130 2011). It was achieved by assimilating surface observations of synoptic pressure into
131 the NCEP GFS model using an Ensemble Kalman Filter variant. Prescribed boundary
132 conditions are HadISST1.1 (Rayner et al. 2003) monthly sea-surface temperature
133 (SST) and sea ice cover data as well as forcing of CO₂, volcanic aerosols and solar
134 radiation.

135 The 20th Century Reanalysis Version 2c (20CRv2c) uses the same model as version 2
136 with new sea ice boundary conditions from the COBE-SST2 (Hirahara et al. 2014),
137 new pentad Simple Ocean Data Assimilation with sparse input (SODAsi.2, Giese et al.
138 2015) sea surface temperature fields, and additional observations from ISPD version
139 3.2.9 (Cram et al. 2015). SODAsi2c is generated by tapering SODAsi.2 at 60° N/S to
140 COBE-SST2 SSTs, which makes the Arctic sea ice and SSTs consistent. For both



141 products, we use the mean of the 56-member ensemble, at a 6-hourly temporal
142 resolution. The spatial resolution corresponds to a Gaussian T62 grid.

143 The ERA-20C (ERA20C) reanalysis (Poli et al. 2016) uses the Integrated Forecast
144 System (IFS) model as a framework to assimilate observations of surface pressure and
145 marine surface winds. It is a global atmospheric reanalysis for the period 1900 – 2010
146 with a 3-hourly temporal resolution and a horizontal resolution of T159 with 91
147 vertical levels, reaching from the surface up to 1 Pa. Sea – ice cover and SST forcing
148 come from an ensemble of realizations (HadISST.2.0.0.0), where the variability in
149 these realizations is based on the uncertainties in the observational sources used for
150 this forcing. The radiation scheme follows exactly the CMIP5 proposal, including
151 aerosols, ozone and greenhouse gases (Hersbach et al. 2015).

152 In addition to the ERA20C reanalysis, the ERA-20C and ERA-Interim (1979-2015)
153 (Dee et al. 2011) land versions (Balsamo et al. 2015) (ERA20CL & ERA-INTERIM-
154 land) are used in our assessment. These land reanalyses consist of off-line runs of the
155 ECMWF land surface model, driven by the atmospheric forcing from the respective
156 reanalysis. When calculating the correlation and root-mean-square error, both the
157 corrected (with GPCP) and uncorrected version of ERA-INTERIM-land are used
158 (referred to ERAINTL-d and ERAINTL-e, respectively). For spatial plots, we only
159 show the corrected version. ERA20C was analyzed in 0.5° resolution, and ERA-
160 INTERIM-land in 1° resolution. It is important to note that none of the atmospheric or
161 land reanalyses used in this study assimilated snow measurements.

162 **2.2 Snow depth observations**

163 This study uses time series of daily snow depths for 820 Russian meteorological
164 stations (distributed as shown in the supplementary Figure 1). The time series are
165 prepared by RIHMI-WDC (All-Russian Research Institute of Hydrometeorological
166 Information—World Data Centre). Meteorological data sets are automatically
167 checked for quality control. Since the procedure of snow observations changed in the
168 past, particular attention was given to the removal of all possible sources of
169 inhomogeneity in the data. However, there have been no changes in the observation
170 procedures since 1965. When using monthly data, we use the maximum snow depth
171 during that month instead of mean value, because it reflects the process of snow



172 accumulation (snow depth is a cumulative and highly inertial characteristic of climate
 173 system). It is especially essential for autumn months when the main processes of snow
 174 accumulation occurs over the territories of Russia.

175 3. Analysis procedure

176 3.1 Choice of long-term daily snow observations

177 Out of the over 800 stations, 15 stations were selected with a record extending back to
 178 the beginning of the 20th century on a daily basis. Stations with records extending
 179 into the 19th century were shortened to start from 1901. All time series end in 2011.
 180 Stations with different starting years are indicated in Table 1. Furthermore, Table 1
 181 displays the location of the 15 stations, including the elevation above sea level. To
 182 correlate daily measurements with daily reanalysis values, values from the closest grid
 183 cell to the station location were chosen. Moreover, the relative amount of missing data
 184 is shown for the each of the three months considered in this study. As can be seen,
 185 data availability differs considerably between months and stations. However, one
 186 station (ID 35108) exceeds 20% missing data in all three months was excluded from
 187 further analysis. We also excluded one station (ID 32098) for which the related grid
 188 box was classified as ocean. This results in a final selection of 13 stations.

189 **Table 1:** 15 long-term snow stations taken out of the Russian snow station data pool.
 190 Listed are WMO ID, name, coordinates, elevation as well as starting year and missing
 191 values. Missing values are indicated relative to the whole sample size of each
 192 individual station for April (A), October (O) and November (N). Red marked stations
 193 where excluded from further analysis.

WMO ID	Station Name	Coordinates	Elevation above sea level	Starting year if not 1901	Missing values in %
22550	Arhangel'sk	64°30' N 40°44' E	8		A (8.8) O (7.9) N (12)
23405	Ust'-Cil'ma	65°26' N 52°16' E	78	1914	A (6.9) O (6.6) N (5.3)
23711	Troicko-Pecherskoe	62°42' N 56°12' E	135		A (5.5) O (6.6) N (6.3)
24641	Viljujsk	63°47' N 121°37' E	110	1903	A (13.5) O (21) N (17.4)
24966	Ust'-Maja	60°23' N 134°27' E	169		A (16.1) O (17) N (17.2)



26063	St. Petersburg	59°23` N 30°18` E	3	1902	A (9.2) O (8) N (16.6)
27199	Kirov	58°36` N 49°38` E	157		A (10.4) O (10.6) N (14)
27675	Poreckoe	55°11` N 46°20` E	136		A (17.5) O (11.7) N (23.2)
27955	Samara (Bezencuk)	52°59` N 49°26` E	45	1904	A (7.7) O (3.5) N (11.3)
28275	Tobol'sk	58°09` N 68°15` E	49	1907	A (17.1) O (17.4) N (23.2)
28440	Ekaterinburg	56°50` N 60°38` E	281		A (5.6) O (2.5) N (3.3)
30758	Chita	52°05` N 113°29` E	671	1926	A (8.3) O (8.1) N (10.4)
32098	Poronajsk	49°13` N 143°06` E	7	1908	A (3.2) O (2) N (8.4)
35108	Urals (Kazakhstan)	51°15` N 51°17` E	37		A (21) O (24.7) N (30.8)
35121	Orenburg	51°41` N 55°06` E	115		A (5.4) O (7.9) N (13.1)

194

195

196 3.2 Calculation of extreme event detection

197 To evaluate the detection rate of extreme daily snow depth events, we calculate the
 198 98th percentile values in all reanalysis products in two different ways. Extreme events
 199 were calculated for both absolute snow depth and accumulated snow depth, the later
 200 being the snow depth difference between two consecutive days. The selected dates in
 201 the reanalyses are then compared to the station dates. Based on the number of dates
 202 selected using station data, a percentage hit-rate is calculated, namely the amount of
 203 extreme events in station data divided by the amount of correctly selected dates in
 204 reanalyses.

205

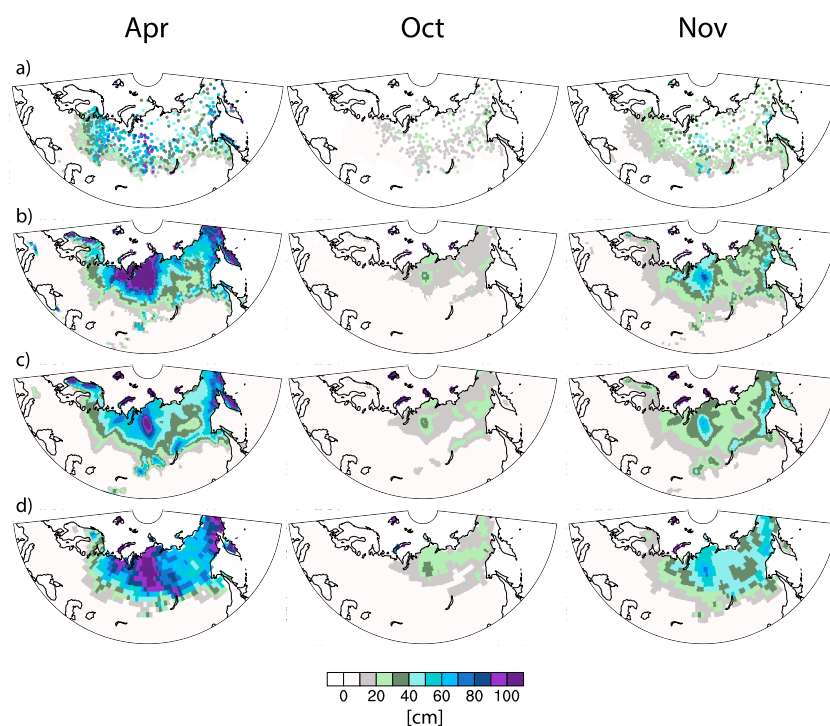
206 4. Results

207 4.1 Spatial features and magnitude

208 While quantitative estimates of how the reanalysis products differ from station data
 209 will be shown later, we first show multi-decadal climatology and tendency maps for a
 210 more qualitative inspection of the snow representation in reanalyses. Starting with the
 211 recent period, Figure 1 shows the snow depth climatology over 1981-2010 for April,



212 October and November. Unsurprisingly, April displays the overall highest values.
 213 Highest snow depths over Eurasia are located in northern Siberia along the 90° E
 214 meridian. Elevated snow depths are also found over the Russian Far East and over
 215 Kamchatka in particular. Both of the features displayed in the station data are also
 216 represented by all reanalysis products. Overall, there is a broad agreement in the
 217 position of high snow depth areas as well as the snow region boundaries. However,
 218 ERA20C shows notably lower snow depths in northern Siberia, compared to ERA-
 219 INTERIM-land and 20CRv2c, but the latter shows generally higher snow depth than
 220 station data, especially in April and November.



221

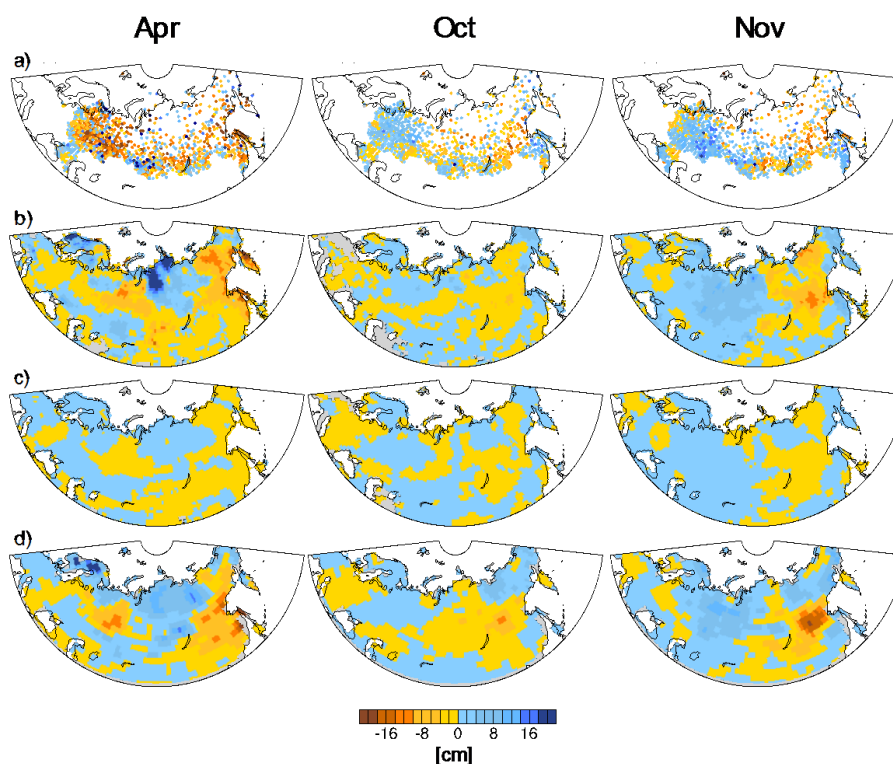
222 Figure 1: 1981-2010 snow depth climatology of (from left to right) April, October and
 223 November in a) observations, b) ERA-INTERIM land-d c) ERA20C and d) 20CRv2c.
 224 ERA20CL, ERA-INTERIM land-e and 20CRv2 are not displayed due to insubstantial
 225 differences to ERA20C, ERA-INTERIM land-d and 20CRv2c.

226 The decadal tendency in the recent era is shown in Figure 2, as snow depth anomalies
 227 between the 1996-2010 period minus those in the 1981-1995 period. In April, the



228 region with strongest snow depth decrease is the western, European part of Russia,
229 west of the Urals and between the Barents and Caspian Sea. This feature is clearly
230 underestimated by all reanalyses, best represented by 20CRv2, followed by ERAINT-
231 1. However, the sign of the tendency is not homogenous over the region in the
232 reanalyses, and local snow depth increases can be found. A second region of snow
233 decrease, which is broadly captured by the reanalyses is the Russian Far East, with
234 ERA20C displaying poorer agreement. A pronounced positive anomaly is found in
235 reanalyses north of Lake Balkhash and extending toward the coasts of the Bara and
236 Laptev Seas, a region where the station coverage is poor though. Towards southern
237 Russia, the observed signal is more complex with snow depth increase towards the
238 border to Kazakhstan, but with snow depth decrease further east on the western side
239 of Lake Baikal, which the gridded products fail to capture, both in terms of extend
240 and magnitude. In autumn, and especially in November, the in-situ data reveal a broad
241 longitudinal dipolar pattern with decrease (increase) of snow depths in the eastern
242 (western) part of Russia, reproduced by the reanalyses.

243 Overall, 20CRv2c captures the observed patterns slightly better than ERA-Interim-
244 land, while ERA20C shows the poorest agreement.



245

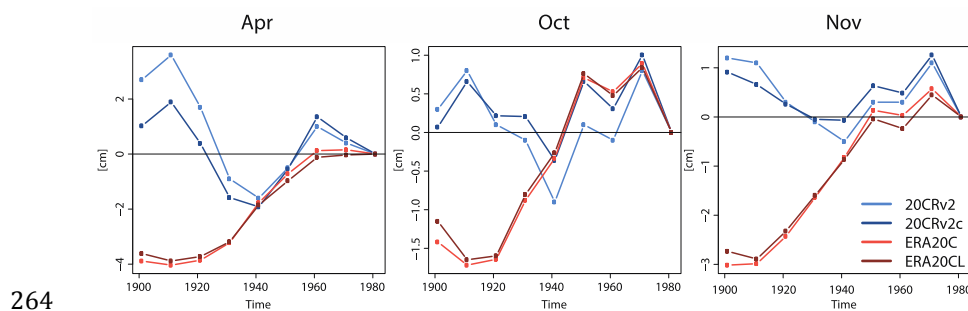
246 Figure 2: 1996-2010 minus 1981-1995 snow depth anomalies of (from left to right)
247 April, October and November in a) observations, b) ERA-INTERIM land-d, c)
248 ERA20C and d) 20CRv2c. ERA20CL, ERA-INTERIM land-e and 20CRv2 are not
249 displayed due to insubstantial differences to ERA20C, ERA-INTERIM land-d and
250 20CRv2c.

251 4.2 Inter-decadal performance

252 Figure 3 shows the long-term decadal changes over the Northern Russia snowpack
253 (averaging between 50°-150° E and 60°-75° N) in the different climate reanalyses.
254 Series of 30-year climatological anomalies were computed with a moving window of
255 10 years, using 1981-2010 period as a reference climatology. From the 1941-1970
256 period onward, all four products show similar tendencies. Further back in time
257 however, the gridded products diverge: ERA20C & ERA20CL continue a downward
258 tendency (mean anomalies decrease) whereas the 20CRv2 & 20CRv2c reanalyses
259 show an overall increase in snow depth, resulting in a notable difference by the early



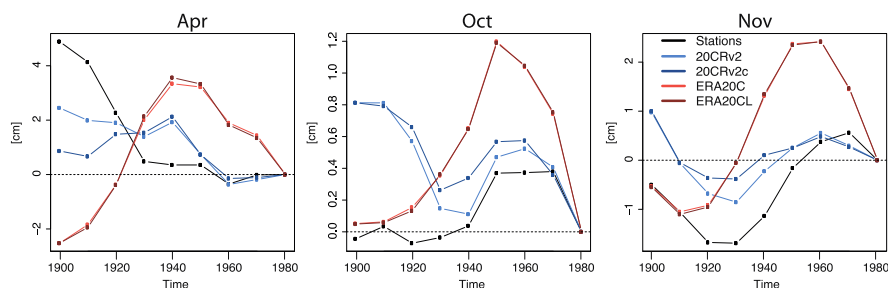
260 20th century. This evolution is, despite minor differences, true for all three months.
261 For all months, the 20CR family of reanalyses show strong positive anomalies for the
262 1911-1940 period, the main period of the Early Twenty Century Arctic Warming
263 (ETCAW).



264

265 Figure 3: Time series of snow depth anomalies in (from left to right) April, October
266 and November averaged over the main northern Russia snow pack (50° - 150° E, 60 -
267 75° N). Each data point represents a 30-year long climatology, starting from 1901-
268 1930 until 1981-2010 with 10 year shifts. Anomalies are calculated relative to the
269 1981-2010 climatology.

270 Unfortunately, none of the 13 selected stations with a long record is located in that
271 northern Russia region. A similar behavior emerges however if the comparison is
272 made between the 13 stations and the collocated reanalysis data, as shown on Figure 4.
273 Again, comparing to the 1981-2010 reference climatology disregards differences in
274 snow depth magnitude and helps focusing on long-term tendencies. All three months
275 show a divergence of the two reanalysis families towards the beginning of the 20th
276 century. Going backward in time from the recent era, tendencies are similar until the
277 1941-1970 period but, afterwards, the ECMWF reanalyses show a declining mean
278 snow depth whereas the 20CR reanalyses favor an increase in snow depth.
279 Interestingly, snow station data agrees very well with the 20CR reanalyses until ca.
280 1951-1980 period, while the ECMWF reanalyses show much more pronounced
281 deviations from the station data anomalies. Towards the beginning of the century, the
282 station data agrees more and more with the ECWFM reanalyses in late autumn, but
283 20CRv2 is closer to station data in April. The ECMWF reanalyses achieve an
284 excellent representation for the 1901-1930 and 1911-1940 periods in autumn (for the
285 1901-1930 spatial anomalies see Supplementary Figure 2).



286

287 Figure 4: Top: Time series of snow depth anomalies in (from left to right) April,
288 October and November for the average of the 13 station locations. Each data point
289 represents a 30-year long climatology, starting from 1901-1930 till 1981-2010 with 10
290 year shifts. Anomalies are calculated relative to the 1981-2010 climatology.

291

292 4.3 Sub-decadal and daily performance

293 Moving away from decadal tendencies, we now evaluate the daily and the inter-
294 annual snow variability over the 13 selected stations with records extending back to
295 the early days of the 20th century. Figure 5 presents the daily performance between
296 station data and the reanalyses over the recent period (1981-2010).

297 The melting season (April) generally exhibits the weakest correlation between grid
298 and station, with slightly better values for October and highest values for November.
299 However, this ranking can differ for individual station locations. For the period 1981-
300 2010, the ERA20C reanalysis achieves better results than the 20CR reanalyses,
301 especially so in April, indicating that melting and temperature evolution is somewhat
302 more accurate in the ECMWF reanalyses. November and even more so October
303 correlations are very similar in all four long-term reanalysis products. As to be
304 expected, the ERA-INTERIM-land reanalysis, given the higher quality of atmospheric
305 forcing in the recent era and the finer spatial resolution, generally scores the highest
306 when compared to the respective station with medians above 0.8 in all three months.
307 Note that in the correlation analysis ERA-INTERIM-land-d achieves higher averaged
308 correlation coefficients than the uncorrected version.

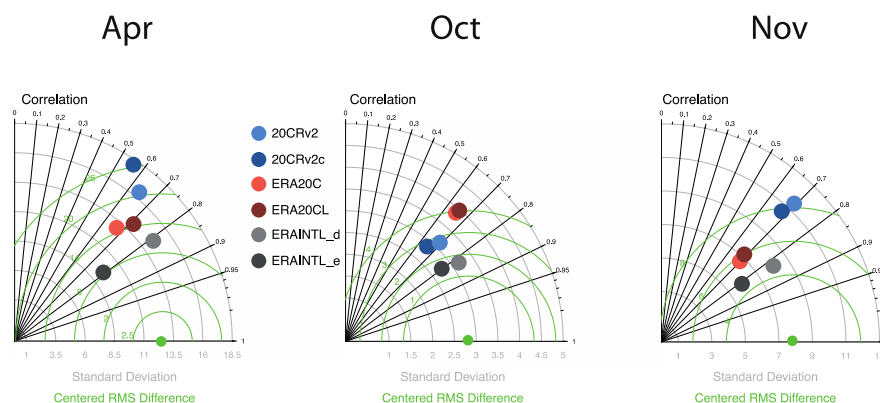
309 Looking at long-term correlations (Figure 6), the ECMWF reanalyses slightly



310 outperform the 20CR in April, but less so than in the 1981-2010 period. The opposite
311 is now true for October, where the 20CRv2 and 20CRv2c achieve slightly higher
312 averaged correlation coefficient values, whereas in November, all long-term
313 reanalyses have comparable correlations with station data with slightly higher values
314 for the 20CR family. In two out of three months, the ERA20C-land version does not
315 realize higher accuracy than the parent product ERA20C. The same is true for the new
316 20CRv2c, which outperforms 20CRv2 only in November.

317 We note that long-term daily correlation coefficients for individual northern stations
318 repeatedly exceed 0.7 (see Supplement Table 1). Only two stations (ID 30758 & ID
319 35121) consistently show very low correlations across the seasons and reanalyses,
320 probably because of their southern positions. In general terms, the linear correlation
321 performance decreases from northern to more southern stations. This reflects the
322 sensitivity of snowfall in relatively mild environments, resulting in short periods of
323 snow availability. Such small-scale snowfall events are hardly captured by the
324 reanalyses.

325 .



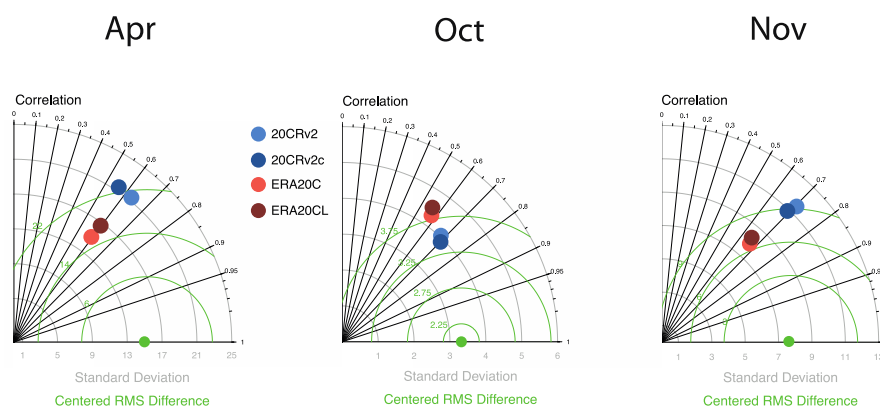
326

327 Figure 5: Taylor diagrams showing the median of the 13 station locations using daily
328 data for the period 1981-2010. The X-axis and Y-Axis indicate the standard deviation,
329 the radians indicate correlation values and the green circles indicate centered RMSE.
330 The green dot shows the observed variability. For more details concerning the
331 datasets statistics, see Supplementary Figures 3-5.



332 Root mean square error (RMSE) values obviously differ from location to location (see
 333 supplement Table 1). Averaging over all stations reanalyses products were found to
 334 produce the absolute largest deviations from the *true* station timeseries in April,
 335 followed by November and lastly October. The low October RMSE is influenced by
 336 the relatively small absolute snow depth values during that month. Thus, even
 337 deviations from zero (e.g. incorrect event of snowfall) will be small. Again, as
 338 expected the ERA-INTERIM land produces the smallest RMSE over all reanalyses.
 339 The ERA-INTERIM land version without the precipitation correction has lower
 340 RMSE in April and November than the version with the precipitation correction. This
 341 could be due to the scarcity and uncertainty of rain-gauge observations in the region,
 342 which would deteriorate the GPCP-based correction. The pair of ERA20C reanalyses
 343 clearly outperforms the 20CR pair in April and November, but is on equal terms in
 344 October.

345



346

347 Figure 6: Taylor diagrams showing the median of the 13 station locations using daily
 348 data for the longest period available (see Table 1). The X-axis and Y-Axis indicate the
 349 standard deviation, the radians indicate correlation values and the green circles
 350 indicate centered RMSE. The green dot shows the observed variability. For more
 351 details concerning the datasets statistics, see Supplementary Figures 3-5.

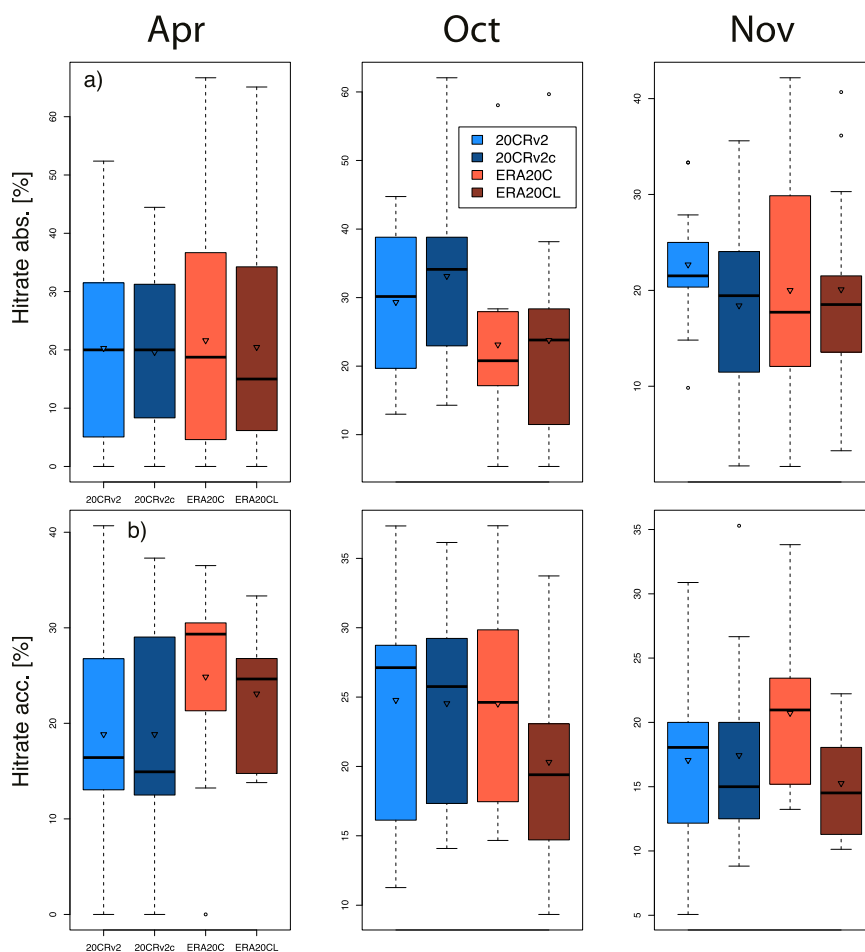
352

353 Finally, to address variability characteristics of the reanalysed snow depth values,
 354 Figure 5&6 (X-axis) also show the median standard deviation of anomaly time series



355 averaged over the 13 stations. As expected, April and November show much higher
356 variability than October. All ECMWF products show a good representation of the
357 station standard deviation. The uncorrected ERA-INTERIM land version apparently
358 suppresses a certain amount of variability with lower median values than the rest of
359 the ECMWF family products. On the other side, both 20CR reanalyses overestimate
360 the variability. October values for 20CRv2 and 20CRv2c are very much influenced by
361 one outlier location, so that the median is still well within the range of the station
362 median.

363 Assessment of variability is especially important in the framework of extreme events.
364 Since the replication of variability and daily correlation seems promising, an extreme
365 event hit-rate is computed to measure how well the reanalysis products can detect the
366 exact dates of extreme events. Figure 7a shows the hit-rate of days with extreme
367 absolute snow depth values whereas Figure 7b shows the hit-rate of days with
368 extreme accumulation of snow depth for the 13 station locations. Better daily
369 correlations in April (Fig. 5) seem to help the ERA20C reanalyses to capture slightly
370 more dates correctly than the two 20CR products. The opposite is true for autumn
371 months, especially for absolute snow depth maxima. Interestingly, changing from
372 absolute to accumulation extremes helps ERA20C to achieve a higher hit-rate,
373 whereas the 20CR products show a slightly worse hit-rate for the latter metric.
374 Moreover, ERA20C land, which shows a very similar if not better performance for
375 absolute snow depth extremes, shows a poorer performance for detecting
376 accumulation extremes. Overall though, mean hit-rates stay well below 40%; only for
377 single locations did the hit-rates exceed 50%.



378

379 Figure 7: Boxplots graphs for the extreme events hitrate analysis of the 13 snow depth
 380 station locations, where the triangle denotes the mean, the bold black line denotes the
 381 median, the box denotes the 25-75% percentile range (or interquartile range), the
 382 whiskers show the upper and lower end or at most the 1.5 x interquartile range and the
 383 dots denote outlier. a) shows boxplots for absolute snow extreme events the longest
 384 possible time period, b) same as a) but for snow accumulation.

385 5. Discussion

386 Comparing snow depths in multiple long-term, centennial reanalyses with in-situ
 387 measurements over Russia, our results indicate a good performance of the reanalysis
 388 datasets. Climatologies are well represented and long-term daily correlations revealed



389 very high coefficient values for most of the station locations. Snow depths from
390 surface input-only reanalyses consistently show linear correlations of 0.6 and higher,
391 although dealing with a very large sample size. Khan et al. 2008 found best case
392 basin-wide correlations of around 0.65 in ERA-40 and JRA-25, with much worse
393 correlations for the NCEP-DOE reanalysis. All these reanalyses assimilated a variety
394 of input data, not only surface data as is the case with the centennial reanalyses
395 examined in this study. Moreover, Khan et al. 2008 state that all evaluated reanalysis
396 snow products showed the worst matching in April.

397 The same result was found in our analysis, where April values showed the smallest
398 correlation and highest absolute error (RMSE). Therefore, it can be assumed that
399 models used for creating the reanalysis datasets still struggle with properly
400 representing melting season (Slater et al. 2001). Looking at the RMSE, it could be
401 shown that the 20CRv2 & 20CRv2c generally overestimate snow depth, and that
402 ERA20C & ERA20CL are closer to the station data. The same applies to the
403 variability comparison. Interestingly, the snow depth RMSE in October is smaller
404 than in the other months, but day-to-day variability (correlation) appears to be better
405 in November. This indicates that the initial snowfall in October, if occurring, is harder
406 to capture than in November, but also generates only small snow depths. Therefore,
407 even if completely missed by the reanalysis, it produced only small RMSEs.

408 Peings et al. 2013 found that 20CRv2 displays a good performance in detecting the
409 daily advance of October and November snow (between 80-100% hitrate). We found
410 that 20CRv2 shows good long-term daily correlations in October and November, even
411 higher than ERA20C. That said, binary snow information as well as correlation
412 analysis masks the details of snow amount, which is better seen in anomaly or
413 climatology maps. Moreover, our hit-rate analysis of dates for extreme snow depths
414 and snow accumulation showed that for the 13 station locations only about 40% of the
415 dates were correctly computed when compared to station data. Among the
416 explanations for this underwhelming performance are a) the assimilation of only
417 surface data in the reanalyses (which challenges the computation of the complex
418 conditions for extreme snowfall), b) the long time frame in which assimilated data
419 quantity is decreasing back in time and c) spatial resolution of the reanalyses which
420 can not resolve features like small scale uplift or orographic precipitation, or at even



421 smaller scale, snowdrift. With these deficiencies in mind, the achieved correlation
422 coefficients for the centennial timeseries are even more remarkable.

423 However, analysis of inter-decadal tendencies of snow depth revealed a peculiar
424 evolution. Generally, the ECMWF datasets compute a stronger snow depth decrease
425 before the 1940s than the 20CR products for the main Russian Arctic snow field.
426 Since climatological maps do not show substantial differences, origin of the large
427 disagreements must emerge in the pre-1950s period. The assimilated input data is near
428 identical between ERA20C and 20CRv2c, and thus model biases seem to be the
429 source of divergence.

430 One reason for the snow depth evolution could be the overestimation of Arctic SLP
431 (sea level pressure) during the pre-1950s in ERA20C (Belleflamme et al. 2015).
432 Indeed we found that ERA20C shows high (higher than 20CR or reconstructed
433 values) positive SLP anomalies for the beginning of the 20th century over Central
434 Russia (see Supplementary Figure 6). Such a high anomaly over the high latitudes
435 might lead to reduced poleward moisture transport, as well as decreased cloud cover
436 and downward long wave radiation, which is very efficient in melting snow.
437 Moreover, stable atmospheric conditions prevent vertical motion and therefore
438 condensation. Knudsen et al. 2015 showed that, in the recent era, both a positive SLP
439 anomaly and a negative anomaly in snowfall prevail over the Russian Arctic coast in
440 summer months with high sea ice melt. Hence, Arctic anti-cyclonic circulation
441 patterns that are associated with sea ice melt also promote low snowfall over the
442 Russian sector of the Arctic, and a similar association could be at play in ERA20C in
443 the pre-1950s. On the other hand, if compared to station data, the ERA20C snow
444 depths show a good agreement for anomalies early in the 20th century.

445 Furthermore, near-surface temperatures influence snow depth evolution. The new
446 20CRv2c dataset uses alternative sea ice and SSTs representations as boundary
447 conditions, which improves the 2m temperature performance over the Arctic
448 compared to 20CRv2. Nevertheless, it is generally still colder than ERA20C or
449 CRUTEMP. However, ERA20C is most probably much too warm during April,
450 whereas the 20CR reanalyses seem to be too cold during November and December,
451 thus they might be overestimating snow depths (see Supplementary Figures 7 and 8).
452 Ultimately, there is no clear and simple answer to this issue and our analysis can only



453 provide an initial assessment of the discrepancy between the two families of
454 reanalyses.

455 The results of the snow climatologies hint towards heterogeneous dataset issues.
456 Decadal tendencies in the second half of the 20th century are better represented by the
457 20CR datasets (relative to their baseline), whereas tendencies for the first half of the
458 century are better represented in ERA20C. Unfortunately, only 13 stations could be
459 used to verify long-term evolution in snow depth. Data recovery from a higher density
460 network with better spatial coverage is needed to really constrain the diverging snow
461 states in these long-term reanalyses. Moreover, future reanalysis or model
462 comparisons might be needed. The planned CERA (ERA20C plus coupled ocean) and
463 GSWP3 could give further insight into this topic. Model inter-comparisons
464 concerning snow representation might reveal necessary qualities to compute a realistic
465 snow depth.

466 **6. Conclusion**

467 Snow depth and its evolution from a variety of centennial reanalyses have been tested
468 against in-situ observations over the Russian territory. Long-term reanalyses are able
469 to reproduce daily and sub-decadal snow depth variability very well. That said,
470 computing the exact day of extreme snow accumulation is still a difficult task for
471 these datasets. Spatially, the region of high and low snow, and the snow cover
472 boundaries are well represented. However, inter-decadal comparison of snow depth
473 revealed some issues with pre-1950s snow climates over northern Russia. The
474 ECMWF and NOAA reanalyses show diverging snow states (low or high,
475 respectively), most probably likely a consequence of assimilation schemes or model
476 biases rather than input data.

477 To further understand and quantify changes during the current and future Arctic warm
478 periods, it is imperative to maintain and expand a dense network of (Arctic) snow
479 measuring stations (including their meta data). Reproducing observed snow (depth) in
480 climate models is a difficult challenge since many environmental factors determine
481 snowfall amount and ultimately snow depth. In-situ snow depth measurements and
482 reanalyses are important tools to evaluate the performance of climate models .

483



484 **Acknowledgments.** YO was supported by the Norwegian Research Council (project
485 SNOWGLACE # 244166 and EPOCASA #229774/E10). AS and SB were supported
486 by the EU-FP7 project ERA-CLIM2 (607029). MW, YO, SB, AS and OB
487 acknowledge funding by the European ERAnet.RUS programme, especially within
488 the project ACPCA.

489

490 **References**

491 Agrawala, S., 2007: Climate change in the European Alps: adapting winter tourism
492 and natural hazards management. Organisation for Economic Cooperation and
493 Development (OECD).

494 Balsamo, G., Albergel, C., Beljaars, A., Boussetta, S., Brun, E., Cloke, H., Dee, D.,
495 Dutra, E., Muñoz-Sabater, J., Pappenberger, F. and P. De Rosnay, 2015: ERA-
496 Interim/Land: a global land surface reanalysis data set. *Hydrology and Earth System*
497 *Sciences*, **19**, 389-407.

498 Barnett, T. P., L. Dümenil, U. Schlese, and E. Roeckner, 1988: The effect of Eurasian
499 snow cover on global climate. *Science*, **239**, 504–507

500 Belleflamme, A., X. Fettweis, and M. Erpicum, 2015: Recent summer Arctic
501 atmospheric circulation anomalies in a historical perspective. *The Cryosphere*, **9**, 53–
502 64.

503 Brown, R. D. and P. W. Mote, 2009: The response of Northern Hemisphere snow
504 cover to a changing climate*. *Journal of Climate*, **22**, 2124–2145.

505 Brown, R., C. Derksen, and L. Wang, 2010: A multidata set analysis of variability and
506 change in Arctic spring snow cover extent, 1967–2008. *Journal of Geophysical*
507 *Research: Atmospheres (1984–2012)*, **115**, D16111.

508 Brown, R. D. and D. A. Robinson, 2011: Northern Hemisphere spring snow cover
509 variability and change over 1922–2010 including an assessment of uncertainty. *The*
510 *Cryosphere*, **5**, 219–229.

511 Brun, E., V. Vionnet, A. Boone, B. Decharme, Y. Peings, R. Valette, F. Karbou, and
512 S. Morin 2013: Simulation of Northern Eurasian Local Snow Depth, Mass, and
513 Density Using a Detailed Snowpack Model and Meteorological Reanalyses, *J.*
514 *Hydrometeorol.*, **14**, 203–219, doi:10.1175/JHM-D-12-012.1.



- 515 Bulygina, O. N., P. Y. Groisman, V. N. Razuvaev, and V. F. Radionov, 2010: Snow
516 cover basal ice layer changes over Northern Eurasia since 1966. *Environmental*
517 *Research Letters*, **5**, 015004.
- 518 Callaghan, T. V., M. Johansson, T. D. Prowse, M. S. Olsen, and L. O. Reiersen, 2011:
519 Arctic cryosphere: changes and impacts. *Ambio*, **40**, 3–5
- 520 Cohen, J. and D. Entekhabi, 1999: Eurasian snow cover variability and Northern
521 Hemisphere climate predictability. *Geophysical Research Letters*, **26**, 345–348.
- 522 Cohen, J. and D. Rind, 1991: The effect of snow cover on the climate. *Journal of*
523 *Climate*, **4**, 689–706
- 524 Cohen, J., J. A. Screen, J. C. Furtado, M. Barlow, D. Whittleston, D. Coumou, J.
525 Francis, K. Dethloff, D. Entekhabi, and J. Overland, 2014: Recent Arctic
526 amplification and extreme mid-latitude weather. *Nature Geoscience*, **7**, 627–637.
- 527 Compo, G.P., Whitaker, J.S., Sardeshmukh, P.D., Matsui, N., Allan, R.J., Yin, X.,
528 Gleason, B.E., Vose, R.S., Rutledge, G., Bessemoulin, P. and S. Brönnimann, 2011:
529 The Twentieth Century Reanalysis project. *Quarterly Journal of the Royal*
530 *Meteorological Society*, **137**, 1–28.
- 531 Cram, T. A., G. P. Compo, X. Yin, R. J. Allan, C. McColl, R. S. Vose, J. S. Whitaker,
532 N. Matsui, L. Ashcroft, R. Auchmann, et al., 2015: The international surface pressure
533 databank version 2. *Geoscience Data Journal*, **2**, 31–46.
- 534 Dee, D. P., S. M. Uppala, A. J. Simmons, P. Berrisford, P. Poli, S. Kobayashi, U.
535 Andrae, M. A. Balmaseda, G. Balsamo, P. Bauer, et al., 2011: The ERA–interim
536 reanalysis: Configuration and performance of the data assimilation system. *Quarterly*
537 *Journal of the Royal Meteorological Society*, **137**, 553–597.
- 538 Flanner, M. G., K. M. Shell, M. Barlage, D. K. Perovich, and M. A. Tschudi, 2011:
539 Radiative forcing and albedo feedback from the Northern Hemisphere cryosphere
540 between 1979 and 2008. *Nature Geoscience*, **4**, 151–155.
- 541 Frei, A. and G. Gong, 2005: Decadal to century scale trends in North American snow
542 extent in coupled atmosphere–ocean general circulation models. *Geophysical*
543 *Research Letters*, **32**, L18502.
- 544 Frei, A., M. Tedesco, S. Lee, J. Foster, D. K. Hall, R. Kelly, and D. A. Robinson,
545 2012: A review of global satellite-derived snow products. *Advances in Space*
546 *Research*, **50**, 1007–1029.



- 547 Ghatak, D., C. Deser, A. Frei, G. Gong, A. Phillips, D. A. Robinson, and J. Stroeve,
548 2012: Simulated Siberian snow cover response to observed Arctic sea ice loss, 1979–
549 2008. *Journal of Geophysical Research: Atmospheres (1984–2012)*, **117**, D23108.
- 550 Giese, B. S., H. F. Seidel, G. P. Compo, and P. D. Sardeshmukh, 2015: An ensemble
551 of historical ocean reanalyses with sparse observational input. *Journal of Geophysical*
552 *Research: Oceans*, **submitted**.
- 553 Hersbach, H., C. Peubey, A. Simmons, P. Berrisford, P. Poli, and D. Dee, 2015: ERA-
554 20CM: a twentieth-century atmospheric model ensemble. *Quarterly Journal of the*
555 *Royal Meteorological Society*.
- 556 Hirahara, S., M. Ishii, and Y. Fukuda, 2014: Centennial-scale sea surface temperature
557 analysis and its uncertainty. *Journal of Climate*, **27**, 57–75.
- 558 Honda, M., J. Inoue, and S. Yamane, 2009: Influence of low Arctic sea-ice minima on
559 anomalously cold Eurasian winters. *Geophysical Research Letters*, **36**, L08707.
- 560 Hüsler, F., T. Jonas, M. Riffler, and J. P. Musial, 2014: A satellite-based snow cover
561 climatology (1985–2011) for the European Alps derived from AVHRR data. *The*
562 *Cryosphere*, **8**, 73.
- 563 Jeong, J.H., H.W. Linderholm, S-H. Woo, C. Folland, B-M. Kim, S-J. Kim and D.
564 Chen 2013: Impact of snow initialization on subseasonal forecasts of surface air
565 temperature for the cold season. *Journal of Climate*, **26**, 1956–1972.
- 566 Jonas, T., C. Rixen, M. Sturm, and V. Stoeckli, 2008: How alpine plant growth is
567 linked to snow cover and climate variability. *Journal of Geophysical Research:*
568 *Biogeosciences (2005–2012)*, **113**, G03013.
- 569 Kanamitsu, M., Ebisuzaki, W., Woollen, J. and Shi-Keng, Y., 2002. Ncep-doe amip-ii
570 reanalysis (r-2). *Bulletin of the American Meteorological Society*, **83**, 1631.
- 571 Khan, V., L. Holko, K. Rubinstein, and M. Breiling, 2008: Snow cover characteristics
572 over the main Russian river basins as represented by reanalyses and measured data.
573 *Journal of Applied Meteorology and Climatology*, **47**, 1819–1833.
- 574 Knudsen, E. M., Y. J. Orsolini, T. Furevik, and K. I. Hodges, 2015: Observed
575 anomalous atmospheric patterns in summers of unusual arctic sea ice melt. *Journal of*
576 *Geophysical Research: Atmospheres*, **120**, 2595–2611.
- 577 Liston, G. E. and C. A. Hiemstra, 2011: The changing cryosphere: Pan-Arctic snow



- 578 trends (1979-2009). *Journal of Climate*, **24**, 5691–5712.
- 579 Onogi, K., J. Tsutsui, H. Koide, M. Sakamoto, S. Kobayashi, H. Hatsushika, T.
580 Matsumoto, N. Yamazaki, H. Kamahori, and K. Takahashi, 2007: The JRA-25 re-
581 analysis. *気象集誌 第2 輯*, **85**, 369–432.
- 582 Orsolini, Y. J. and N. G. Kvamstø, 2009: Role of Eurasian snow cover in wintertime
583 circulation: Decadal simulations forced with satellite observations. *Journal of*
584 *Geophysical Research: Atmospheres (1984–2012)*, **114**, D19108.
- 585 Orsolini, Y. J., R. Senan, G. Balsamo, F. J. Doblas-Reyes, F. Vitart, A. Weisheimer,
586 A. Carrasco, and R. E. Benestad, 2013: Impact of snow initialization on subseasonal
587 forecasts. *Climate Dynamics*, **41**, 1969–1982.
- 588 Park, H., J. E. Walsh, Y. Kim, T. Nakai, and T. Ohata, 2013: The role of declining
589 Arctic sea ice in recent decreasing terrestrial Arctic snow depths. *Polar Science*, **7**,
590 174–187.
- 591 Peings, Y., E. Brun, V. Mauvais, and H. Douville, 2013: How stationary is the
592 relationship between Siberian snow and Arctic Oscillation over the 20th century?
593 *Geophysical Research Letters*, **40**, 183–188.
- 594 Peñuelas, J., T. Rutishauser, and I. Filella, 2009: Phenology feedbacks on climate
595 change. *Science*, **324**, 887.
- 596 Poli, P., H. Hersbach, D. P. Dee, A. J. Simmons, F. Vitart, P. Laloyaux, D. G. H. Tan,
597 C. Peubey, J.-N. Thépaut, Y. Trémolet, E. V. Hólm, M. Bonavita, L. Isaksen, and M.
598 Fisher 2016: ERA-20C: An Atmospheric Reanalysis of the Twentieth Century.
599 *Journal of Climate*, **29**, 4083-4097.
- 600 Rayner, N. A., D. E. Parker, E. B. Horton, C. K. Folland, L. V. Alexander, D. P.
601 Rowell, E. C. Kent, and A. Kaplan, 2003: Global analyses of sea surface temperature,
602 sea ice, and night marine air temperature since the late nineteenth century. *Journal of*
603 *Geophysical Research: Atmospheres (1984–2012)*, **108**, 4407.
- 604 Rienecker, M. M., M. J. Suarez, R. Gelaro, R. Todling, J. Bacmeister, E. Liu, M. G.
605 Bosilovich, S. D. Schubert, L. Takacs, and G.-K. Kim, 2011: MERRA: NASA’s
606 modern-era retrospective analysis for research and applications. *Journal of Climate*,
607 **24**, 3624–3648.
- 608 Siljamo, N. and O. Hyvärinen, 2011: New geostationary satellite-based snow-cover
609 algorithm. *Journal of Applied Meteorology and Climatology*, **50**, 1275–1290.



- 610 Slater, A. G., C. A. Schlosser, C. Desborough, A. Pitman, A. Henderson-Sellers, A.
611 Robock, K. Y. Vinnikov, J. Entin, K. Mitchell, F. Chen, et al., 2001: The
612 representation of snow in land surface schemes: Results from pilps 2 (d). *Journal of*
613 *Hydrometeorology*, **2**, 7–25.
- 614 Uppala, S. M., P. W. Kållberg, A. J. Simmons, U. Andrae, V. Bechtold, M. Fiorino, J.
615 K. Gibson, J. Haseler, A. Hernandez, and G. A. Kelly, 2005: The ERA-40 reanalysis.
616 *Quarterly Journal of the Royal Meteorological Society*, **131**, 2961–3012.
- 617 Wegmann, M., Y. Orsolini, M. Vázquez, L. Gimeno, R. Nieto, O. Bulygina, R. Jaiser,
618 D. Handorf, A. Rinke, and K. Dethloff, 2015: Arctic moisture source for Eurasian
619 snow cover variations in autumn. *Environmental Research Letters*, **10**, 054015.
- 620 Wu, R., G. Liu, and Z. Ping, 2014: Contrasting Eurasian spring and summer climate
621 anomalies associated with western and eastern Eurasian spring snow cover changes.
622 *Journal of Geophysical Research: Atmospheres*, **119**, 7410–7424.
- 623 Yasunari, T., Kitoh, A. and Tokioka, T., 1991: Local and remote responses to
624 excessive snow mass over Eurasia appearing in the northern spring and summer
625 climate—a study with the MRI GCM. *J. Meteor. Soc. Japan*, **4**, 473–487.
- 626 Ye, K., R. Wu, and Y. Liu, 2015: Interdecadal change of Eurasian snow, surface
627 temperature, and atmospheric circulation in the late 1980s. *Journal of Geophysical*
628 *Research: Atmospheres*, **120**, 2738–2753.
- 629 Zhang, X., J. He, J. Zhang, I. Polyakov, R. u. d. Gerdes, J. Inoue, and P. Wu, 2013:
630 Enhanced poleward moisture transport and amplified northern high-latitude wetting
631 trend. *Nature Climate Change*, **3**, 47–51.
- 632 Zuo, Z., S. Yang, R. Zhang, D. Xiao, D. Guo, and L. Ma, 2015: Response of summer
633 rainfall over China to spring snow anomalies over Siberia in the NCEP CFSv2
634 reforecast. *Quarterly Journal of the Royal Meteorological Society*, **141**, 939–944.